

# Development of Multimode Gas Fired Combined Cycle Chemical-Looping Combustion Based Power Plant Lay-Outs

Basavaraja Revappa Jayadevappa (✉ [basavarajarj@rvce.edu.in](mailto:basavarajarj@rvce.edu.in))

RV College of Engineering <https://orcid.org/0000-0002-4853-1551>

---

## Research Article

**Keywords:** chemical looping combustion, lay-out, gaseous fuels, energy balance, multimode, carbon capture.

**Posted Date:** August 19th, 2021

**DOI:** <https://doi.org/10.21203/rs.3.rs-735652/v1>

**License:**  This work is licensed under a Creative Commons Attribution 4.0 International License.

[Read Full License](#)

---



38 **Declarations**

39 **Ethics approval and consent to participate:** No human/animals data are being used for the research  
40 work.

41 **Consent for publication:** Not applicable

42 **Availability of data and materials:** Not applicable.

43 **Competing interests:** The authors declare that they have no competing interests

44 **Funding:** This research work has not funded by government/private agencies or institutions.

45 **Authors' contributions:** Complete work involved in literature findings, heat/mass balances, power  
46 cycle calculations, layout development was being done by the single author Basavaraja R J

47

48

49

50

51

52

53

54

55

56

57

58

59

60

61

62

63

64

65

66

67

68



104 **NOTATION**

105	CLC	Chemical-looping combustion
106	CC	Combined cycle
107	HRSG	Heat recovery steam generator
108	IGCC	Integrated gasification combined cycle
109	SMOC	Steam moderated oxyfuel combustion
110	$h_{\text{Air in}}$	Enthalpy in air entering into air reactor, kJ/kg
111	$h_{\text{Dep Air}}$	Enthalpy of oxygen depleted air reactor leaving the system, kJ/kg
112	$h_{\text{MeO}}$	Enthalpy in oxygenated carrier, kJ/kg
113	$h_{\text{Me}_{x-1}}$	Enthalpy in reduced oxygen carrier, kJ/kg
114	$h_{\text{Fuel in}}$	Enthalpy flow in fuel entering fuel reactor, kJ/kg
115	$h_{\text{Exhaust}}$	Enthalpy flow in exhaust leaving fuel reactor, kJ/kg
116	$\Delta H_{\text{Ox}}$	Heat of oxidation, kJ/mol
117	$\Delta H_{\text{Red}}$	Heat of reduction, kJ/mol
118	$M_{\text{Exhaust}}$	Mass flow of exhaust (containing CO <sub>2</sub> and water vapor) leaving fuel reactor per unit time, kg/s
119	$M_{\text{O}_2\text{in}}$	Mass of oxygen in fresh air, entering to air reactor, kg/s
120	$M_{\text{Dep Air}}$	Mass of depleted air at the exit of air reactor, kg/s
121	$M_{\text{O}_2\text{out}}$	Mass of oxygen present in depleted air at the exit of the air reactor, kg/s
122	$M_{\text{Fuel in}}$	Mass of fuel entering into fuel reactor, kg/s
123	$M_{\text{Exhaust}}$	Mass of exhaust gas (containing CO <sub>2</sub> and water vapor) leaving fuel reactor respectively, kg/s
124	$M_{\text{MeO}_x}$	Mass of oxidized oxygen carrier, kg/s
125	$M_{\text{MeO}_{x-1}}$	Mass of reduced oxygen carrier, kg/s
126	$P_1$	Compressor inlet pressure, bar
127	$P_2$	Compressor outlet pressure, bar
128	$r_p$	Compression pressure ratio
129	$T$	Temperature at any point, °C
130	$T_1$	Temperature of the gas at compressor inlet, K
131	$T_{2s}$	Isentropic temperature of gas at compressor exit, K
132	$T_3$	Temperature of the fluid at gas turbine inlet and, K
133	$T_{4s}$	Isentropic temperature at gas turbine exit respectively, K
134	$\gamma$	Specific heat capacity ratio

135

136

137

138

139

## 140 1. INTRODUCTION

141 Emission of greenhouse gas primarily carbon dioxide from power stations is a major concern for energy sectors,  
142 climate change and terrestrial ecosystem (IPCC, 2014; IPCC, 2020). At present, carbon dioxide emission from  
143 power sectors alone is 35-40 % of the total CO<sub>2</sub> emission and in these sectors fossil fuels accounts for the  
144 anthropogenic CO<sub>2</sub> emissions. Carbon dioxide concentration was increased in last one decade with an average  
145 growth of 2.4 ppm/year and the 2020 concentration of CO<sub>2</sub> is 415 ppm and CO<sub>2</sub> emissions is about 60 % higher  
146 compared to last 160 years (IEA, 2016; IEA, 2021). The various options in reducing emission of carbon to the  
147 atmosphere is focused by many advanced combustion technologies and major research and concern is on: (i)  
148 increasing efficiency by reducing energy consumption; (ii) use of less carbon emissive fuel; (iii) storage of CO<sub>2</sub>  
149 using biological absorption methods in forest and soils (IPCC,2005; IPCC, 2007). The most of combustion  
150 technologies involve energy penalty in flue gas cleaning and subsequent carbon capture. This should be  
151 minimized to implement CCS with least energy penalty. There are several advantages with gas fuels (for  
152 example natural gas and syngas) over high carbon emissive solid fuels to make power generation less CO<sub>2</sub>-  
153 intensive. The dependency of coal based power generation will continue in countries like India, China and South  
154 Africa for the next 40 years (Jayanti et al., 2012).

155  
156 Emissions of carbon dioxide from the power plants and industries have been great interest in by means of  
157 carbon captured and sequestration (CCS) (IPCC, 2014). Three principal way to capture CO<sub>2</sub> from flue gas upon  
158 combustion in power plants; these are post-combustion capture, pre-combustion capture and oxyfuel combustion  
159 (Ghoniem and Needs, 2011). Comparative analysis of natural gas fired oxyfuel and CLC based power plant  
160 lay-outs is made by Basavaraja and Jayanti (2015a) and net efficiency reported for oxyfuel based CC CO<sub>2</sub>  
161 recycle and combined cycle steam moderated oxyfuel combustion (CC SMOC) is respectively 30.93 % and  
162 46.57 % and CLC atmospheric and CC CLC is respectively 43.11% and 51.94% after incorporating energy  
163 penalty for CO<sub>2</sub> compression to 110bar. Though state of art has been illustrated in these technologies with  
164 technical maturity (Wall 2007), many of these involves energy penalty in CO<sub>2</sub> capture. Energy penalty for coal  
165 based, post capture and compression is 12%, oxyfuel combustion capture is 11.2%, IGCC Shell is 9.4% and  
166 NGCC post combustion capture is 5.8 %(Davison and Thambimuthu, 2009).

167  
168 Existing power plants needs CCS with well-planned retrofitting. Development of present power plant with the  
169 provision of CCS entails additional capital investment. Raymond et al. (2014) studied on retrofitting power

170 plant for carbon sequestration and problems associated with carbon constrained energy planning (CCEP).  
171 Operation of power plant with CCS involves number of factors like fuel type, electricity cost, and geographical  
172 area for sequestration and environmental issues (Tola and Pettinau, 2014). A detailed analysis on fuel switching  
173 for CLC based power plant layout was made by Basavaraja and Jayanti (2015b) to address alternative fuel as  
174 energy source for atmospheric CLC plants by thermodynamic, transport and kinetic factors considerations. Oxy-  
175 coal based combustion is gaining attention in research, Jayanti and Kareemulla (2016) studied on the low  
176 temperature flashing for simultaneous CO<sub>2</sub> and SO<sub>2</sub> capture in oxy coal combustion based power plants. There  
177 is a need for combustion technology that enables power plant is to be operated in both CCS and non-CCS mode.  
178 Combustion in power plant based on CLC enables plant to operate with or without capture of CO<sub>2</sub> with  
179 minimum retrofit.

180

181 The concept of Chemical-looping combustion was proposed in 1954 to produce pure CO<sub>2</sub> and later research  
182 work to increase thermal efficiency on reversibility of combustion processes using chemical-looping concept is  
183 made (Lewis and Gilliland., 1954; Richter and Knoche., 1983; Ishida et al. , 1987 and Jin and Ishida., 1994).  
184 The important parameters of CLC based plants, such as gas-solid contact pattern, oxygen carrier reactivity at  
185 different temperatures for various fuels and temperature distribution in reactor system, are now well understood  
186 by research (Adanez et al., 2012; Mansoor et al., 2017; Sumana et al. 2020, Jun and Xiang., 2021).

187 Technically mature Rankine-cycle type oxyfuel-combustion based power plants show 10 to 12% (Jayanti et al.,  
188 2012; Jenni et al., 2013; Navajas et al., 2019) energy penalty even though thermal losses can be minimized by  
189 proper design and optimization of power cycle. A studies on CLC based power plants show that energy loss  
190 will be minimal (Naqvi, 2006; Kvamsdal, 2007; Navajas et al., 2019) in oxygen separation from air and such  
191 studies made in integrated gasification combined cycle (IGCC) power plant with and without CO<sub>2</sub> capture  
192 (Petrescu and carmos, 2017). Pressurized CLC show higher thermal efficiency and there has been possibility of  
193 operating in both CCS and non CCS modes. Jin and Ishida (2006), Abad et al.(2007) and Adanaz et al. (2006)  
194 studied on kinetics of oxygen carriers in pressurized CLC environment in lab scale. These results cannot be used  
195 to scale-up reactor but these show kinetics in 1 to 15 bar range CLC system will be feasible in case of heavy  
196 duty CLC reactors. These studies shows operating CLC based units with high thermal efficiency without much  
197 energy consumption for air separation with the feasibility of handling flue gas in CCS and non-CCS mode.  
198 While studies on pressurized/combined cycle based CLC system operation (Naqvi 2006; Wolf 2004; Zang

199 2018) have been reported in literature, detailed combined cycle CLC based power plant lay-out with an option  
200 to handle flue gas with CO<sub>2</sub> capture and free let-out have not properly addressed .

201 The objective of this work is to develop gas fired power plant lay-out incorporating two ways of handling flue  
202 gas with a prospective to know heat generation sections and heat utilization to generate electrical power using  
203 Brayton and Rankine cycles while still ensuring options of handling flue gas containing CO<sub>2</sub> in CCS and non  
204 CCS routes.

205 This paper aims to study, develop process flow sheet and analyse two gas fired pressurized chemical-looping  
206 combustion power plants and their configuration for two modes of operations i.e., one with carbon capture mode  
207 and other one is allowing flue gas from plant to atmosphere thereby enabling retrofitting possibility for fuel  
208 switch.

209 Three power plants based on pressurized chemical-looping combustion are considered and are :

210 (a) a natural gas fueled plant with and without carbon capture modes, (b) a syngas fueled plant with and  
211 without carbon capture modes, and (c) a future ready plant operating with and without carbon capture  
212 modes with an retrofit for an option to fuel switch.

213

## 214 **2. DEPICTION OF MASS AND ENERGY CALCULATION**

### 215 **2.1 Pressurized Chemical Looping Combustion**

216 The principle of pressurized chemical looping combustion is shown in Figure 1. Here, the fuel combustion is  
217 split in two stages. Firstly, a solid metal (in a low oxidation state, denoted as MeO<sub>x-1</sub>) is oxidised by oxygen in  
218 the air to form metal oxide (completely oxidized state, denoted as MeO<sub>x</sub>) in air reactor. In the later stage, the  
219 metal oxide gives oxygen to react with the hydrocarbon fuel during fluidization to form carbon dioxide and  
220 water vapor in fuel reactor. Two stage combustion of fuel by reactor systems eliminates oxygen separation unit  
221 and avoids mixing of N<sub>2</sub> with flue gas. The exit gases from CLC reactor system are taken through gas turbines  
222 followed by heat recovery steam generators to generate power and CO<sub>2</sub> separated from the flue gas upon cooling  
223 sent for compression.

224 Pressurised operation of CLC reactor systems enables combined power cycles operated under gas turbine as per  
225 Brayton cycle and steam turbine as per Rankine cycle to get improved net thermal efficiency of power plant

226 (Kehlhofer, 1999; El-Wakil, 2010). In recent years, pressurized CLC is gaining importance from the researches  
227 in the view of reactor configuration, solid-gas contact, reaction kinetics, fuel conversion (Abad et al., 2007; Xiao  
228 et al., 2010; Xiao et al., 2012; Zheng et al., 2014). Studies made by Adanez et al. (2006) and Garcia-Labiano et  
229 al. (2006) shows that reduction of NiO to Ni oxygen carrier conversion remains 100% for CH<sub>4</sub>, H<sub>2</sub>, CO and O<sub>2</sub>  
230 and conversion is reduced at higher pressure. This decrease in the solid conversion is typically in the range of  
231 16-30 bar ranges and therefore in the present work we have chosen 13 bar pressure as highest gas pressure (at  
232 depleted air turbine) at Brayton cycle. In the pilot plant studies (Erlach et al., 2011) showed no attrition and no  
233 agglomeration when that Ni/NiO can be operated at 1300°C in CLC units. Temperature and pressure for air  
234 turbine of the Brayton cycle are fixed at 1200°C and 13bar, respectively.

235

236 The heat required for the endothermic metal oxide reduction (by fuel) is supplied from the oxidized metal  
237 coming from air reactor. Reaction in two CLC reactors is by gas-solid contact during fluidization. Based on  
238 reactive nature of oxygen carrier with air and fuel, air reactor operates in circulating fluidized bed mode and fuel  
239 reactor operates in bubbling fluidized bed mode. Due to varying type of fluidization in air and fuel reactors  
240 results more pressure drop and to account for this pressure in the fuel reactor is assumed to be 11.5 bar (at  
241 1150°C) with the solid conversion of 80%. Similar condition (Naqvi, 2006; Adanez et al. 2006) used in  
242 literature for pressurized CLC systems. We have chosen this operating pressure for realistic operation of CLC  
243 reactor system. The gases expanded to one bar from gas (air and exhaust) turbine are further cooled by heat  
244 recovery steam generators to run steam turbines of Rankine cycle and water preheaters to preheat feed water.  
245 Cooled depleted air let to atmosphere. Exhaust gas containing water vapor is separated CO<sub>2</sub> upon cooling in flue  
246 gas conditioner and more than 95% pure CO<sub>2</sub> is compressed to a pressure of 110 bar for sequestration. Two  
247 possible way of handling flue gas from CLC plant unit is shown in Figure 2, one without capturing CO<sub>2</sub> and  
248 another one with power consumption carbon. The energy balance and combined cycle arrangement is discussed  
249 in section 2.2.

250

## 251 **2.2 Energy balance**

252 In this section mass and energy balance details for the combined cycle CLC system are given. The Nickel oxide  
253 (NiO) supported on Nickel di-aluminium tetroxide (NiAl<sub>2</sub>O<sub>4</sub>) in a 60:40 weight ratio is chosen as oxygen  
254 carrier. The nickel oxide flow rate calculation is made by considering 25% excess oxygen supply to fuel in fuel

255 reactor. The CLC-reactors are assumed to be adiabatic with isothermal and homogenous mixing of solids with  
 256 gases. Air flow rate is calculation is considered in air reactor with an  $\sim 220\%$  of an excess air. Considering  
 257 major components of the natural gas and syngas fuels, and their reaction with NiO is given as per reactions (1),  
 258 (2) and (3) respectively with excess oxygen (Adanez et al., 2012):



262 Nickel is oxidized to nickel oxide in air reactor as per reaction (4) given below



264 In reactions (1) to (4), values of heat of reaction shown has been estimated from the values available in literature  
 265 (Adanez et al., 2012; Linderholm et al., 2008) for the temperature range  $1150^\circ\text{C}$  to  $1230^\circ\text{C}$ . Based on reactions  
 266 (1) to (4) stoichiometric oxygen requirement for syngas is calculated and in similar way other components of  
 267 natural gas is estimated. One can see here that syngas composition consist major portions of carbon monoxide,  
 268 hydrogen and lessor part of methane. Reaction of CO and  $\text{H}_2$  with NiO is exothermic compared to lessor  
 269 methane gas endothermic reaction with NiO. This make overall syngas reaction with NiO as mildly exothermic.

270  
 271 In this system, power is generated primarily by Brayton cycle and bottoming Rankine cycle. The basis for all  
 272 CLC calculations is amount of fuel converted in the reduction/fuel reactor. In combined cycle CLC, metal  
 273 oxidation reaction is taken up by large mass of excess air. With given fuel flow, the amount of oxygen converted  
 274 is found from reaction stoichiometry, and the heat balance for the air reactor can be solved. Air and fuel reactors  
 275 heat balance (as per Figure 3) is formulated respectively according to Eqs. (5) and (6):

276  
 277  $M_{\text{Air in}} h_{\text{Air in}} + M_{\text{MeO}_{x-1}} h_{\text{Me}_{x-1}} + (M_{\text{O}_2\text{in}} - M_{\text{O}_2\text{out}}) \Delta H_{\text{Ox}} = M_{\text{Dep Air}} h_{\text{Dep Air}} + M_{\text{MeO}} h_{\text{MeO}}$  (5)

278  
 279  $M_{\text{Fuel in}} h_{\text{Fuel in}} + M_{\text{MeO}_x} h_{\text{MeO}} - M_{\text{Fuel in}} \Delta H_{\text{Red}} = M_{\text{Exhaust}} h_{\text{Exhaust}} + M_{\text{MeO}_{x-1}} h_{\text{Me}_{x-1}}$  (6)

280  
 281 In Eq. (5), terms  $h_{\text{MeO}}$ ,  $h_{\text{Me}_{x-1}}$ ,  $h_{\text{Air in}}$ ,  $h_{\text{Dep Air}}$  are, respectively, the enthalpy in oxidized metal, reduced metal  
 282 , air entering and oxygen depleted air leaving the air reactor. In Eq. (6), terms  $h_{\text{Fuel in}}$  and  $h_{\text{Exhaust}}$  are  
 283 respectively, the enthalpy of fuel entering into fuel reactor and enthalpy of exhaust (stream containing  $\text{CO}_2$  and

284 water vapor).  $\Delta H_{Ox}$  is the heat of oxidation in kJ/mol i.e., heat released during reaction of Ni with  $O_2$  to form  
285 NiO . The term  $\Delta H_{Red}$  is heat of reduction in kJ/mol i.e., heat absorbed during the natural gas oxidation or NiO  
286 reduction. Ni oxidation is exothermic reaction and therefore the term  $\Delta H_{Ox}$  associated with molar mass is with  
287 plus sign as given in Eq. (5) and NiO reduction in fuel reactor is endothermic for the natural gas fired case and  
288 thus the term  $\Delta H_{Red}$  associated with molar mass is with minus sign as given in Eq. (6) and same will be become  
289 plus sign for exothermic NiO reaction with syngas. Here  $M_{O_2in}$ ,  $M_{Dep Air}$ ,  $M_{O_2out}$ ,  $M_{Fuel in}$ ,  $M_{Exhaust}$  are  
290 respectively mass of oxygen in the fresh air, mass of the depleted air, unreacted or excess oxygen leaving air  
291 reactor, mass of fuel entering into fuel reactor and mass of exhaust gas (containing  $CO_2$  and water vapor)  
292 leaving fuel reactor respectively. In Eqs.(5) and (6),  $M_{MeO_x}$  and  $M_{MeO_{x-1}}$  denotes oxidized and reduced states of  
293 oxygen carrier respectively.

294  
295

### 296 **2.3 Pressurized chemical-looping combustion power cycle**

297

298 A schematic diagram of the pressurized CLC power cycle is shown in Figure 4. The CLC Brayton cycle consists  
299 of air compressor, depleted air turbine and exhaust gas ( $CO_2+H_2O$ ) turbine. The fuel is assumed to be  
300 pressurized. The oxygen depleted air from the air reactor and exhaust stream containing  $CO_2$  and water vapor  
301 from the fuel reactor are drawn into two separate Brayton cycles and are expanded in an air turbine and  $CO_2$   
302 turbine. The CLC reactor exit gases after expansion preheats the respective reactor inlet gases using gas-gas  
303 heat exchangers or recuperators. The heat left in the exhaust and depleted gas streams is extracted by using  
304 series of heat exchangers or heat recovery steam generators (HRSG) to generate steam as per Rankine cycle.  
305 Figure 4 shows combined cycle chemical looping combustion power cycle arrangement having two Brayton  
306 cycles and a Rankine cycle.

307

## 308 **3. RESULTS AND DISCUSSION**

309 Thermal input for natural and syngas fired combined cycle CLC based power plant is considered as  $761 MW_{th}$   
310 and  $800 MW_{th}$  respectively, supplied in continuous fuel flow. The composition in mole % of natural gas  
311 (Linderholm et al. 2009) is taken as 89.51%  $CH_4$ , 5.92%  $C_2H_6$ , 2.36%  $C_3H_8$ , 0.40% isobutene, 0.56% n-butane,  
312 0.13% isopentane, 0.08% n-pentane, 0.06%  $C_6H_{12}$ , 0.28%  $N_2$  and 0.70  $CO_2$  with lower heating value of 49.17  
313 MJ/kg. Syngas ( that generates almost two times the quantity of  $CO_2$  of that of natural gas upon complete

314 combustion) molar composition (Winslow 1977) is taken to be 45.7% H<sub>2</sub>, 19.6% CO, 6.6% CH<sub>4</sub> and 28.1%  
315 CO<sub>2</sub> with the lower heating value of 11.2 MJ/kg.

316 In both fuel fired case, comprehensive mass and energy balance is made and thermodynamic analysis is carried  
317 on the gas preheaters, air reactor, the fuel reactor, gas turbines (depleted air and exhaust gas turbines) of Brayton  
318 power cycle and steam turbines of Rankin power cycles. The results from these calculations are discussed  
319 below.

### 320 **3.1 Lay-out of Natural Gas Fired Pressurised CLC**

321 In this section detailed mass and energy balance for power plant and complete process flow sheet of pressurized  
322 CLC plant is discussed and details of these are given below.

#### 323 **3.1.1 Mass and Energy Balances**

324 Mass and heat balances are made on CLC reactor system conating five major CLC sub-units. These are the fuel  
325 oxidation reactor (operating at 1150°C and 11.6 bar), the air oxidation reactor (operating at 1200°C and 13 bar),  
326 the fuel and the air pre-heaters and coolant air flow. Mass flow of individual stream of these sub-units has been  
327 found by balancing moles of reactant and product based on the fuel component mole fractions. Using Eqs. (5)  
328 and (6) heat (energy) balances have been made for natural gas fueled combined cycle CLC system of 761 MW<sub>th</sub>  
329 fuel input. The resulting energy and mass flow rates in and out of these sub-units are shown in Figure 5.

330

331 Compressed air (at 177°C and 13.5 bar) at mass flow of 870.12 kg/s is divides into two streams namely coolant  
332 air flow of 58.44 kg/s and the process air of 811.68 kg/s. Air of mass flow 811.68 kg/s (with 215.55 % excess  
333 O<sub>2</sub>) is drawn to the CLC reactor system and heated air (at 420°C) from recuperator enters air reactor where 59.7  
334 kg/s of oxygen present in the air is selectively reacted with metal (containing of 218.95 kg/s of Ni, 69.66 kg/s of  
335 NiO and 232.21 kg/s of NiAl<sub>2</sub>O<sub>4</sub>) to form metal oxide stream (containing of 348.31 kg/s of NiO and 232.21 kg/s  
336 of NiAl<sub>2</sub>O<sub>4</sub>). Conversion of NiO to Ni is 80% in the fuel reactor. The Energy produced by exothermic metal  
337 oxidation reaction in the air is taken out by N<sub>2</sub> rich air (of flow 751.99 kg/s) and metal oxide streams. The heat  
338 absorbed by endothermic metal oxide reduction reaction in fuel reactor is 113 MW. This is supplied by the  
339 oxygen carrier. 15.47 kg/s of natural gas is preheated from 30 to 350°C by the exhaust gas of 75.1 kg/s. The O<sub>2</sub>-  
340 depleted air from the air reactor is 751.99 kg/s at 1200°C. The oxygen depleted air and coolant air (58.44 kg/s at  
341 177°C) mix at the turbine inlet to form a total mass flow of 810.43 kg/s and a temperature of 1132°C at the  
342 turbine inlet. The depleted air and coolant bleed mixture gases expand in the gas turbine. The depleted air

343 turbine exit gas temperature at 1 bar is 497°C. Exhaust gas temperature reduces to 666°C upon expansion.  
344 The computed value  $\gamma (= C_p/C_v)$  for oxygen depleted air and fuel reactor exhaust given are 1.345 and 1.226,  
345 respectively. These values are comparable with these reputed literatures (Naqvi et al., 2007; Wolf, 2004) for  
346 same inlet gas composition for depleted air and exhaust turbines. Depleted air at the exit of air reactor (at  
347 1200°C) mixes with the coolant air so that turbine inlet temperature is taken to be 1132°C. Turbine efficiency  
348 ( $\eta_t$ ) is taken in the range of 91-92% (Wolf, 2004) and a value of 92% is used in the present studies. Nearly  
349 atmospheric pressure depleted air and exhaust gas streams (after expansion in gas turbines) at low pressure are  
350 used for power generation (as per Ranking Cycle) after preheating respective reactor inlet gases. The complete  
351 process description for the combined cycle chemical-looping combustion power plant flow diagram is given  
352 below (section 3.1.2).

353

### 354 **3.1.2 Natural gas Fired Power plant lay-out**

355 Chemical-looping combustion based combined cycle is unique compared to a conventional combined cycle as  
356 the depleted air from the air reactor and flue gas containing CO<sub>2</sub> and water vapor from the fuel reactor are drawn  
357 into two separate Brayton cycles and are expanded in an air turbine and CO<sub>2</sub> turbine. Combined cycle chemical-  
358 looping combustion power cycle consists of four major components namely compressor, recuperators, gas  
359 turbine and steam turbine.

360

361 Since combustion is divided into oxidation and reduction reactions in two pressurized fluidized bed reactors,  
362 therefore two gas turbines are used to expand them in the proposed lay-out. Gases are compressed to desired  
363 reactors operation using compressors. Recuperators provide necessary heat to preheat the reactants. Description  
364 of the streams in the process plant as shown in Figure 6 is described below.

365

366 The terms A1, A2, A3 denote fresh air streams and are respectively air before compression, air after first stage  
367 of compression and air at the exit of second compression stage. Major part of the compressed air (A4) is first  
368 preheated and then admitted to the air reactor to oxidise the reduced metal oxide (M2). The depleted air (A7)  
369 mixes with the cooling air (A5) drawn from air compressor and then expands down. The depleted air from the  
370 turbine exit (A8) preheats the fresh air (A4) to (A6). The depleted air from the turbine exit is further cooled from  
371 A9 to A10 by water stream (S8) to generate steam (S9). Pressurized fuel (F1) after preheating (F2) reacts with  
372 the oxygenated metal carrier (M1) to form CO<sub>2</sub> and H<sub>2</sub>O vapour mixture exhaust (E1). The expanded exhaust

373 (E2) from the turbine preheats the fuel by cooling down to (E3) and further cools down (E4) by giving heat to  
374 water stream S2 which form steam S3. The depleted air stream finally cools to 75°C (A10 to A11) while  
375 heating water stream (S5) to stream (S6). Thus, the exit gases from air turbine and exhaust gas are drawn into  
376 Rankine cycle through heat recovery steam generator to generate subcritical steam at 190°C (1.7 bar). The  
377 exhaust gas stream at 128°C is let to the atmosphere through chimney when power plant operates in without  
378 CO<sub>2</sub> mode. To operate power plant in carbon capture mode as shown in Figure 7, the exhaust stream from fuel  
379 reactor is admitted to flue gas conditioner for further cooling to ~40°C and the condensed water vapour is  
380 separated (E6) and CO<sub>2</sub> gas (E7) is compressed to 110 bar (E8) at 35°C. The isentropic efficiency of gas and  
381 steam turbines are assumed to be 92%. Thermodynamic analysis of the natural gas fueled CC CLC is shown in  
382 the Table 1. The efficiency of water pump and compressor are taken as 75% and 85% respectively.

383

### 384 **3.2 Lay-out of Syngas Fired Pressurised CLC**

385 Mass and Energy balance model is same as already presented in Section 3.1.1 for pressurized CLC with natural  
386 gas as the fuel has been used to determine the furnace side parameters for syngas firing. Since syngas has  
387 higher cost of compression of CO<sub>2</sub>, the lay-out has been designed for a 800 MW<sub>th</sub>, which amounts to 71.43 kg/s  
388 of syngas flow and is 4.6 higher than the flow rate of natural gas required for a 761 MW<sub>th</sub> plant. On the furnace  
389 side, the principal sub-systems considered are the air reactor and its preheater, the fuel reactor and its preheater,  
390 the gas turbines used to extract power from these exhausts and the compressor to supply air to the air reactors as  
391 well as coolant air to the air turbine. Syngas is assumed to be available under pressurized conditions and the  
392 cost of its compression is not included in the analysis. As in the case of syngas, the air reactor is fixed to  
393 operate at 13 bar and 1200°C, and the fuel reactor is fixed to operate at the pressure of 11.6 bar (at 1226°C).  
394 The same oxygen carrier is used and its flow rate has been determined for syngas requirements for an 800 MW<sub>th</sub>  
395 power plant. The operating temperature of the fuel reactor and the inlet and exit temperatures of the  
396 recuperators have been adjusted to account for the exothermicity of the reduction reaction in the syngas-fired  
397 fuel reactor. The specific heat capacity ratio ( $\gamma$ ) is taken as 1.20. The resulting mass and energy flow rates into  
398 these subsystems are shown in Figure 8.

399

400 The process flow diagram for the CC CLC is shown in the Figure 9. Description of the streams in the process  
401 plant is briefly explained below. The inlet and exit streams reactor system is same as natural gas layout. The  
402 energy utilization from exit gas of the syngas fired power plant is given below. The expanded exhaust (E2) from

403 the gas turbine gets cooled down to E3 in the processing preheating the fuel and further to E4 and E5 by giving  
404 heat to water stream S2 to form high pressure steam S3 which is superheated to S4 by the cooling exhaust gas  
405 (E5 to E6). After expansion in the high pressure turbine (S5), the exit steam is reheated (S6) and fed to the  
406 medium pressure (20 bar) steam turbine. After expansion to 1.7 bar in the medium pressure turbine, it is mixed  
407 with steam generated in various sections (S3, S6 and S16) of process the plant from O<sub>2</sub>-depleted air and exhaust  
408 gas steams via heat recovery steam generators to produce superheated steam at 1.7 bar at a temperature 190°C.  
409 It then finally expands from 190° to 39°C (at 0.069 bar). The exhaust gas (E6) at temperature 128°C leaves the  
410 plant through chimney to atmosphere. The thermodynamic properties of the streams at various locations is  
411 shown in Thermodynamic analysis of the CC CLC is shown in the Table 2.

412

### 413 **3.3 Schematic Diagram of the non-CCS and CCS enabled modes Power Plant**

414 A schematic diagram of the proposed power cycle is shown in Figure 4. It is based on pressurized chemical  
415 looping combustion of gaseous hydrocarbon fuels such as natural gas, syngas, biogas and shale gas. The  
416 combustion of the hydrocarbon fuels occurs in two stages in two separate reactors. In the fuel reactor, the fuel  
417 combusts with a metal oxide, e.g., NiO supported on NiAl<sub>2</sub>O<sub>4</sub> in a 60:40 weight ratio (taken in present work)  
418 prepared in the form of micron-sized particles, and gets converted to CO<sub>2</sub> and H<sub>2</sub>O. In the process, the metal  
419 oxide gets reduced. It is therefore fed to the air reactor where it gets regenerated by reacting directly with air.  
420 Both the metal oxidation and the metal reduction reactions are carried in the range of 1150 to 1250°C,  
421 depending on the reaction and on the fuel. A circulating fluidized bed type of configuration is envisaged for the  
422 cyclic oxidation/ reduction reactions of the metal/metal oxide. It is also proposed that the reactions are carried  
423 out at a pressure of 13 bar in the air reactor and at a slightly reduced pressure of 12 bar in the fuel reactor. The  
424 high temperature reactions in the reactors thus give rise to high temperature gaseous products at a pressure of 12  
425 to 13 bar. These are expanded in separate air or gas turbines to near atmospheric pressure. The expanded gases  
426 will still be hot having a temperature of 500 to 700°C depending on the reactor and the fuel. These are then used  
427 partly to preheat the gaseous reactants and partly to generate a Rankine cycle to generate further electrical  
428 power. In the process of giving up heat for the Rankine cycle, the oxygen-depleted air from the air reactor gets  
429 cooled down to ~120°C and is fed to a chimney as it contains little CO<sub>2</sub>. The exhaust from the fuel reactor too  
430 gets cooled down to ~100°C as it passes through the heat recovery systems. For the CCS mode of operation of  
431 the power plant the exhaust stream (E6) is admitted into the flue gas conditioner where it is finally cooled to  
432 40°C (E5). The condensed water vapour is separated (E6) and CO<sub>2</sub> gas (E7) is compressed to 110 bar (E8) at

433 35°C if CCS is mandatory or let into the atmosphere through the air chimney when CCS need not be  
434 implemented as shown in Figure 10.

435

436 Specific features of the lay-out that make it advantageous and future-ready are:

- 437 • the use of a combined cycle operation to ensures high power output
- 438 • The use of chemical looping combustion mode of burning of hydrocarbon fuel enables CO<sub>2</sub> capture as  
439 a built-in feature.
- 440 • The in-built feature of CO<sub>2</sub> capture enables the power plant to be ready for CCS when it becomes  
441 mandatory. At that stage, minor changes in the gas flow path, after it gets cooled to ~100°C, are  
442 required and a provision to compress CO<sub>2</sub> to 110 bar must be made. Thus, the retrofitting to implement  
443 CCS would be minimal.
- 444 • By proper sizing of the major equipment, it is possible for the plant to be used with as widely different  
445 fuels as methane-rich natural gas (or shale gas) and CO/H<sub>2</sub>-rich syngas (or biogas).

446

447 These aspects are elaborated further below.

448 A process flow diagram of the proposed power plant lay-out is shown in Figure 9. Based on mass and energy  
449 balances discussed in sections 3.1 and 3.2, this has been developed for a 761 MW<sub>th</sub> plant when fired with natural  
450 gas and 800 MW<sub>th</sub> when fired with syngas. Major have now been identified and the flow paths of the various  
451 material streams, such as air, hydrocarbon fuel, steam and metal oxide, have been identified. Process flow  
452 sheeting calculations have been done for four different modes of operation, namely, with natural gas firing with  
453 and without CCS, and with syngas firing with and without CCS and the pressure, temperature and flow rate at  
454 several important locations in the flow paths have been calculated. These are summarized in Table 3. The fact  
455 that the same lay-out descriptors can be used for all four configurations highlights the multi-mode capability of  
456 the plant design. The two specific features, namely, dual fuel flexibility and readiness for CCS, engender small  
457 changes in the process stream flow paths. These have been identified in Figure 9. Fuel switching from syngas  
458 to natural gas requires the fuel reactor exhaust stream to go directly from E3 to E5, thus bypassing the high  
459 pressure and the medium pressure turbines of the Rankine cycle system. There should be a corresponding  
460 bypassing of the relevant heat recovery steam generators by the water on the steam side. Switching from a non-  
461 CCS mode (which is the current practice) to CCS mode (which may be required in future) requires the fuel

462 reactor exhaust to be sent to CO<sub>2</sub> compressor via a exhaust gas cooler to remove steam instead of being sent to  
463 the air chimney.

464

465 Finally, the overall efficiency of the power plant under various modes of operation is summarized in Table 3.  
466 Here, a listing is made of the various processes by which power is produced and those by which power is  
467 consumed for the four configurations.

468 Overall energy analysis is made for power plant lay-outs and net efficiency for each case is evaluated using Eq.  
469 (7) considering the energy penalties for gas compression and water circulation.

$$470 \eta_{\text{Net}} = \frac{P_{\text{Net CC CLC}}}{m_{\text{fuel}} \cdot Q_{\text{LHV}}} \quad (7)$$

471

472 In Eq. (7),  $\eta_{\text{Net}}$  is net efficiency of power plant,  $m_{\text{fuel}}$  is mass flow rate of fuel in kg/s,  $Q_{\text{LHV}}$  is lower heating  
473 value (kJ/kg) of the fuel and  $P_{\text{Net CC CLC}}$  is net power available for combined cycle chemical looping combustion  
474 power plant and  $P_{\text{Net CC CLC}}$  evaluated using Eq. (8)

$$475 P_{\text{Net CC CLC}} = P_{\text{CO}_2+\text{Air}+\text{steam}} - P_{\text{Air comp}} - P_{\text{CO}_2 \text{ comp}} - P_{\text{water pump}} \quad (8)$$

476

477 In Eq. (8),  $P_{\text{CO}_2+\text{Air}+\text{steam}}$  is power produced (kW) by CO<sub>2</sub>/exhaust, air and steam turbines,  $P_{\text{Air comp}}$  and  
478  $P_{\text{CO}_2 \text{ comp}}$  is respectively power consumed (kW) by air and CO<sub>2</sub> compressors and  $P_{\text{water pump}}$  is power  
479 consumed (kW) to pump water.

480

481 It can be seen that with CCS, a net thermal efficiency of 52.13% is obtained with natural gas and 48.78% with  
482 syngas using Eqs. (7-8). In the non-CCS mode (without CO<sub>2</sub> compression), higher thermal efficiencies of 54.06  
483 % and 52.63% efficiencies are obtained. The lower difference between the natural gas and the syngas in the  
484 non-CCS mode is reflective of the higher rate of CO<sub>2</sub> generation in the latter per MW<sub>th</sub> of the fuel. The high  
485 efficiencies obtained in all these cases are partly due to combined cycle operation, partly due to the use of  
486 supercritical boilers in the steam cycles and partly due to the use of chemical looping combustion as opposed to  
487 oxyfuel combustion. It may be noted that in these calculations, allowance has been made for non-idealities in  
488 the expansion, compression and pumping processes involving fluid flow. Allowance has also been made for the  
489 power required to compress CO<sub>2</sub> to a pressure of 110 bar so that the nearly pure (purity > 99%) can be sent to a  
490 CO<sub>2</sub> sequestration/ storage/ reuse site.

491

492 Thus, it can be concluded the above power plant, which offers operational flexibility coupled with high  
493 efficiency, has the necessary attributes of a future-ready power plant producing power from conventional  
494 hydrocarbon fuels in an environmentally friendly way.

495

### 496 **3.4 Assessment of Possibility of Dual Fuel Operation**

497 In order to assess the possibility of dual fuel operation of the pressurized CLC system, a detailed comparison of  
498 several parameters associated with the two systems is made Table 4. It can be seen that most of the parameters  
499 are fairly similar; the operating temperature of the fuel reactors are slightly different. Due to the exothermicity  
500 of the reduction reaction, the fuel reactor temperature is actually higher than that of the air reactor by about  
501 26°C with syngas, whereas it is lower by about 50°C in the case of natural gas firing. Another difference  
502 between the two fuels is the calorific value and the fuel gas flow rate. Since syngas contains significant amount  
503 of CO<sub>2</sub> as inert, its flow rate is higher and the flow rate of the exhaust gas from the fuel reactor is also higher.  
504 This, coupled with the higher exit temperature of the fuel reactor and lesser gas preheating requirement, results  
505 in significantly higher amount of thermal power (105.64 MW for syngas vs 51.71 MW for natural gas) retained  
506 in the fuel reactor exhaust gas (see Figure 5 and Figure 8) which is available for powering a Rankine cycle. As  
507 can be seen from Table 4, the Rankine cycle for syngas has three turbines (a high pressure turbine (150 bar), a  
508 medium pressure turbine (20 bar) and a low pressure turbine (1.7 bar)) while the one for natural gas has a single  
509 low pressure turbine with a turbine inlet pressure of 1.7 bar.

510 It can be seen that the major part of the power is produced by the low pressure turbine in the syngas case and  
511 that its rating is roughly the same (33,216 kW<sub>e</sub> to 29,396 kW<sub>e</sub>) as that of the low pressure turbine in the natural  
512 gas case. The air reactor side parameters are nearly similar and there is hardly 5% change in the heat and mass  
513 flow rates of various streams. From the above reasoning, it can be argued that except for minor changes in the  
514 lay-out for the Rankine cycle parameters, the lay-outs of the syngas-fired and the natural gas-fired pressurized  
515 CLC power plants are similar and a unified lay-out is produced in Figure 10. In this common lay-out, natural  
516 gas firing requires by-passing of the fuel reactor exhaust from E3 to E6 directly. Correspondingly, the steam  
517 side too bypasses the high pressure and the medium pressure turbines and uses only the low pressure turbine.  
518 The stream values corresponding to the unified lay-out are given in Table 1 for natural gas and Table 2 for  
519 syngas firing. These represent only minor departures from the normal settings and can be re-engineered without  
520 significant difficulty. This means that the thermodynamic compatibility between syngas and natural gas lay-  
521 outs for pressurized CLC can be achieved without significant retrofitting. The reaction engineering and

522 transport phenomena considerations are similar to those already as our earlier work (Basavaraja and Jayanti,  
523 2015b). While the kinetics of pressurized oxidation/ reduction reactors have not been fully worked out, it  
524 appears that the kinetics of all the reactions are slowed down in a similar way in the pressure ranges considered  
525 (Adanez et al., 2012; Garcia-Labiano et al. 2006). As demonstrated in our earlier work (Basavaraja and Jayanti,  
526 2015b), the fluidization and heat transfer compatibility conditions can be met by careful design of the relevant  
527 equipment. Thus, it appears that dual fuel flexibility can be incorporated into pressured CLC lay-out at the  
528 design stage itself. In the Table 4, work reported by Naqvi and his co-workers (2007) for 697,545 kW thermal  
529 input natural gas fired pressurised CLC plant operates at 1200°C (13 bar) at air reactor and 980°C (11.6 bar) at  
530 fuel reactor. The oxygen carriers, operating pressure (at air and CO<sub>2</sub> turbines), compressor efficiency chosen is  
531 same as reported by Naqvi and his co-workers (2007) for the natural gas fired CC CLC plant layout calculations  
532 of the present work with 761,000 kW thermal input and the net efficiency is found to be 52.13% and which is  
533 comparable net efficiency reported by Naqvi and his co-workers (2007). The detailed analyses of CC CLC  
534 reactor operating conditions, power produced at gas and steam turbines, power consumed for air and CO<sub>2</sub>  
535 compression, net efficiencies are shown in Table 4.

536

#### 537 **4. FUTURE-READINESS OF THE LAY-OUT**

538

539 The lifetime of a thermal power plant is in excess of 50 years. While carbon capture and sequestration is not  
540 mandatory right now, it is possible that it may become so in a decade or two. In this scenario, it is necessary to  
541 build power plants that are future-ready, i.e., which can be made to operate in a case where CCS becomes  
542 mandatory. Extensive retrofitting of the power plant to accommodate carbon capture may not be possible and  
543 should be avoided. From the future-compatibility point of view, a chemical looping combustion-based power  
544 plant is clearly the superior design. CLC plants can work in either CCS mode or non-CCS mode with very little  
545 changes required to make the switch. No special efforts or equipment will be necessary to enable CO<sub>2</sub> capture.  
546 If CCS is not needed, then the flue gas from the flue gas conditioner need not be compressed and can be sent  
547 directly to the chimney. When CCS is required, then this flue gas can be diverted to a CO<sub>2</sub> compressor. In the  
548 case of a power plant based on oxyfuel combustion, more extensive changes are required as an air separation  
549 unit is required for generating pure oxygen. While studies (Jayanti et al. 2012) indicate that retrofitting of  
550 atmospheric air combustion coal-fired boilers for working in oxyfuel mode, is possible, the case for pressurized  
551 oxyfuel combustion may be different because flue gas compression and recirculation are necessary. In the case

552 of pressurized oxyfuel combustion, the flow rates and composition of the exhaust gas are significantly different  
553 from those under air combustion; this may warrant changes in the turbine and heat recovery systems.

554

## 555 5. CONCLUSION

556 In the present study, analysis of two modes of operation of two gas fired pressurised chemical-looping  
557 combustion based power plant has been made. The principle conclusions drawn from the study is given:

558 • From the detailed mass and heat balances and thermodynamic analysis, power plant lay-outs have been  
559 prepared for pressurised CLC based power plant for fuels natural gas and syngas.

560 • Two modes of power plant operation, one not requiring CCS (the present day mode) and one requiring  
561 CCS (in a future scenario), have been considered within the ambit of pressurized CLC-based power  
562 plant. It is shown that since CLC generates CO<sub>2</sub>-rich flue gas (contains CO<sub>2</sub> and water vapor only)  
563 which is ready for sequestration, the power plant can be readily operated in a dual mode with a loss of  
564 2% of net thermal efficiency with natural gas and up to 4% for syngas.

565 • A single lay-out of future-ready power plant offering in-built CO<sub>2</sub> capture, high efficiency and fuel  
566 flexibility has been developed for power generation using gaseous hydrocarbon fuels.

567 • Oxyfuel combustion based power plants are technically mature in terms of proven commercial scale  
568 operation of new elements. They also have competitive net thermal efficiency if pressurised steam  
569 moderated oxyfuel combustion (SMOC)-based oxyfuel combustion is used. However, they make a  
570 poor choice in terms of future readiness of fuel/equipment flexibility and may warrant significant  
571 retrofitting effort to make them CCS-compatible. CLC plants can work in either CCS mode or non-  
572 CCS mode with very little changes required to make the switch.

573

574

575

576

577

578

579

580

581

582

583

584

585

586

587

588 **REFERENCES**

- 589 Abad A, Adánez J, García-Labiano F, Diego LFD, Gayán P, Celaya J. Mapping of the range of operational  
590 conditions for Cu-, Fe-, and Ni-based oxygen carriers in chemical-looping combustion. *Chem Eng Sci*  
591 2007;62:533–49.
- 592 Abad A, Adánez J, García-Labiano F, Diego LFD, Gayán P, Celaya J. Mapping of the range of operational  
593 conditions for Cu-, Fe-, and Ni-based oxygen carriers in chemical-looping combustion. *Chem Eng Sci*  
594 2007;62:533–49.
- 595 Adanez J, Abad A, Garcia-Labiano F, Gayan P. Diego LFD. Progress in chemical-looping combustion and  
596 reforming technologies. *Prog Energy Combust Sci.* 2012;38:215–82.
- 597 Adanez J, Garcia-Labiano F, DiegoLFD, Gayan P, Celaya J, Abad, A. Nickel-copper oxygen carriers to reach  
598 zero CO and H<sub>2</sub> emissions in chemical-looping combustion. *Ind Eng Chem Res* 2006;45:2617-2625.
- 599 Adanez, J., Gayan, P., Celaya, J., de Diego, L. F., Garcia-Labiano F. and Abad, A. Chemical Looping  
600 combustion in a 10kWth prototype using a CuO/Al<sub>2</sub>O<sub>3</sub> oxygen carrier: Effect of operating conditions on  
601 Methane combustion. *Ind. Eng. Chem. Res.* 2006; 45:6075-6080.
- 602 Basavaraj R. J., Jayanti S. Syngas-fueled, chemical-looping combustion-based power plant lay-out for clean  
603 energy generation. *Clean Technol and Environ Policy* 2015c;17:237-247.
- 604 Basavaraja, R. J. and Jayanti, S. Comparative Analysis of four Gas-Fired, Carbon Capture-enabled Power Plant  
605 Lay-outs. *J. Clean Technol. and Environ* 2015a;17:2143-2156.
- 606 Basavaraja, R. J. and Jayanti, S. Viability of Fuel Switching of a Gas-fired Power Plant Operating in Chemical-  
607 Looping Combustion Mode. *Energy* 2015b;81: 213-221.
- 608 Brandvoll O, Bolland O. (2004). Inherent CO<sub>2</sub> capture by using chemical looping combustion in a natural gas  
609 fired power cycle. *J. Eng. Gas Turbines Power*, 126:316-321.
- 610 Davison J and Thambimuthu K. An overview of technologies and costs for carbon dioxide capture in power  
611 plants. *Proc I Mech E Part A: J Power Energy* 2009; 223:201–212.
- 612 El-Wakil, Mohamed M. *Power Plant Technology*. 3rd ed. New Delhi: Tata McGraw Hill; 2010, India.
- 613 Erlach B, Schmidt M, Tsatsaronis G. Comparison of carbon capture IGCC with pre-combustion decarbonisation  
614 and with chemical-looping combustion. *Energy* 2011; 36:3804–15.
- 615 G. Zang, J. Jia, S. Tejasvi, A. Ratner, E.S. Lora. Techno-economic comparative analysis of biomass integrated  
616 gasification combined cycles with and without CO<sub>2</sub> capture *International Journal of Greenhouse Gas Control*  
617 2018, 78:73-84.
- 618 Garcia-Labiano F, Adanez J, Diego LFD, Gayan P, Abad A. Effect of Pressure on the Behavior of Copper-,  
619 Iron-, and Nickel-Based Oxygen Carriers for Chemical-Looping Combustion *Energy Fuels* 2006;1:26–33.
- 620 Ghoniem, A. F. Needs, resources and climate change: clean and efficient conversion technologies. *Progress in*  
621 *Energy and Combustion Science* 2011; 37: 15-51.
- 622 IEA (2016). IEA statistics: CO<sub>2</sub> emissions from fuel combustion, International Energy Agency, Paris, France.
- 623 IEA (2021), Net Zero by 2050, IEA, Paris <https://www.iea.org/reports/net-zero-by-2050>.
- 624 IPCC (2007). *Climate Change 2007: Synthesis Report*. Contribution of working groups I, II and III to the  
625 Fourth Assessment Report of the Intergovernmental Panel on Climate Change. IPCC, Geneva, Switzerland.
- 626 IPCC (2014). *Climate Change 2014: Synthesis Report*. Contribution of working groups I, II and III to the Fifth  
627 Assessment Report of the Intergovernmental Panel on Climate Change. IPCC, Geneva, Switzerland.
- 628 IPCC (2019): *Climate Change and Land: an IPCC special report on climate change, desertification, land*  
629 *degradation, sustainable land management, food security, and greenhouse gas fluxes in terrestrial ecosystems*.  
630 IPCC, Geneva, Switzerland. In press.

- 631 IPCC special report on carbon dioxide capture and storage. Cambridge, UK: Cambridge University Press; 2005.
- 632 Ishida M, Zheng D, Akehata T. Evaluation of a chemical-looping combustion power-generation system by  
633 graphic exergy analysis. *Energy* 1987, 2: 147–154.
- 634 Ishida, M. and Jin H. A new advanced power-generation system using chemical-looping combustion. *Energy*  
635 1994 19:415–422.
- 636 J Wolf, CO<sub>2</sub> Mitigation in Advanced Power Cycles- Chemical Looping Combustion and Steam-Based  
637 Gasification. Doctoral Thesis: Royal Institute of Technology; 2004.
- 638 Jayanti S and Kareemulla, D. Detailed plant layout studies of oxy-enriched CO<sub>2</sub> pulverized coal combustion-  
639 based power plant with CO<sub>2</sub> enrichment. *J. Clean Technol. and Environ* 2016;18:1985-1996.
- 640 Jayanti S, Saravanan V, and Sivaji S. Assessment of retrofitting possibility of an Indian pulverized coal boiler  
641 for operation with Indian coals in oxy-coal combustion mode with CO<sub>2</sub> sequestration. *Proc. I Mech E Part A: J*  
642 *Power Energy* 2012;226:1003–1013.
- 643 Jenni KE, Baker ED, Nemet JF. Expert elicitations of energy penalties for carbon capture technologies. *Int J*  
644 *Greenhouse Gas Control* 2013;12: 136–45.
- 645 Jin H, Ishida M. Reactivity study on a novel hydrogen fueled chemical-looping combustion. *Int J Hydrogen*  
646 *Energy* 2001;26: 889–894.
- 647 Jun Hu Shiyi and Chen Wenguo Xiang. Ni, Co and Cu-promoted iron-based oxygen carriers in methane-fueled  
648 chemical looping hydrogen generation process. *Fuel Process Techn*, 2021; 221: 106917
- 649 Kehlhofer RH. Combined cycle gas and steam turbine power plants. 2nd ed. Oklahoma: Penn Well; 1999.
- 650 Kvamsdal HM, Jordal K, Bolland O. A quantitative comparison of gas turbine cycles with CO<sub>2</sub> capture. *Energy*  
651 2007;32:10–24.
- 652 Letitia Petrescu, Calin-Cristian Cormos. Environmental assessment of IGCC power plants with pre-  
653 combustion CO<sub>2</sub> capture by chemical & calcium looping methods. *J. Clean. Production* 2017; 158:233-244.  
654 <https://doi.org/10.1016/j.jclepro.2017.05.011>
- 655 Lewis WK., and Gilliland ER (1954). Production of pure carbon dioxide. US Patent 2665972.
- 656 Linderholm C, Abad A, Lyngfelt A, Mattisson T. 160 h of chemical-looping combustion in a 10 kW reactor  
657 system with a NiO-based oxygen carrier. *Int J Greenh Gas Control* 2008; 2:520–530.
- 658 Linderholm, C., Mattisson, T. and Lyngfelt, A. Long-term integrity testing of spray dried particles in a 10kW  
659 chemical-looping combustor using natural gas as fuel. *Fuel* 2009; 88: 2083-2096.
- 660 Mansour Mohammedramadan Tijani, Aqsha Aqsha, Nader Mahinpey. Synthesis and study of metal-based  
661 oxygen carriers(Cu, Co, Fe, Ni) and their interaction with supported metal oxides (Al<sub>2</sub>O<sub>3</sub>, CeO<sub>2</sub>, TiO<sub>2</sub>, ZrO<sub>2</sub>)  
662 in a chemical looping combustion system, *Energy* 2017; 138:873–882.
- 663 Naqvi, R., Wolf, J. and Bolland, O. Part load analysis of a chemical looping combustion combined cycle for  
664 CO<sub>2</sub> capture. *Energy* 2007; 32: 360–370.
- 665 Navajas et al. Life cycle assessment of natural gas fuelled power plants based on chemical looping combustion  
666 technology. *Energy Conversion and Management* 2019;111856.  
667 <https://doi.org/10.1016/j.enconman.2019.111856>
- 668 Ooi REH, Foo DCY and Tan RR. Targeting for carbon sequestration retrofit planning in the power generation  
669 sector for multi-period problems. *Applied Energy* 2014;113:477–87.
- 670 Richter HJ, Knoche KF. Reversibility of combustion processes. ACS Symposium Series 1983; 71-85.
- 671 Shadab Alam J, Pradeep Kumar K, Yamuna Rani, C Sumana. Comparative assessment of performances of  
672 different oxygen carriers in a chemical looping combustion coupled intensified reforming process through

673 simulation study-A review. *Journal of Cleaner Production* 2020; 262:121146.  
674 <https://doi.org/10.1016/j.jclepro.2020.121146>

675 Tola V, Pettinau A. Power generation plants with carbon capture and storage : A techno-economic comparison  
676 between coal combustion and gasification technologies. *Applied Energy* 2014;113:1461–74.

677 Wall TF. Combustion processes for carbon capture. *Proc. Combust. Inst.* 2007; 31, 31–47.

678 Winslow. A. M. (1977). Numerical model of coal gasification in a packed bed. Symposium (international) on  
679 combustion. **16**, 503–513.

680 Xiao R, Chen LY, Saha C, Zhang S, Bhattacharya S. Pressurized chemical-looping combustion of coal using an  
681 iron ore as oxygen carrier in a pilot-scale unit. *Int J Greenh Gas control* 2012;10:363-73.

682 Xiao R, Song QL, Zhang SA, Zheng WG, Yang YC. Pressurized chemical-looping combustion of Chinese  
683 bituminous coal: cyclic performance and characterization of iron ore-based oxygen carrier. *Energy Fuel*  
684 2010;24:1449-63.

685 Zheng, M., Shen, L. and Feng, X. In situ gasification chemical looping combustion of a coal using the binary  
686 oxygen carrier natural anhydrite ore and natural iron ore. *Energy Convers Manag* 2014; 83:270-283.

687

688

689

690

691

692

693

694

695

696

697

698

699

700

701

702

703

704

705

706

707

708

709 **LIST OF FIGURES**

710 Figure 1: Schematic illustration of pressurized chemical-looping combustion

711 Figure 2: Schematic of flue gas handling in proposed chemical-looping combustion based power plant  
712

713 Figure 3: Schematic of energy flow in combined cycle chemical-looping combustion  
714

715 Figure 4: Arrangement of combined cycle CLC power cycle  
716

717 Figure 5: Furnace side heat balance of 761 MW<sub>th</sub> natural gas fueled combined cycle chemical looping  
718 combustion plant  
719

720 Figure 6: Schematic of natural gas fueled combined cycle chemical-looping combustion power plant  
721 without the provision for carbon capture  
722

723 Figure 7: Schematic of natural gas fired 761 MW<sub>th</sub> combined cycle chemical-looping combustion power  
724 plant with provision of carbon capture  
725

726 Figure 8: Furnace side heat balance for 800 MW<sub>th</sub> syngas fueled combined cycle CLC based power  
727 plant  
728

729 Figure 9: Schematic of syngas fueled combined cycle chemical-looping combustion power plant  
730 without the provision for carbon capture  
731

732 Figure 10: Schematic diagram of multi-fuel compatible combined cycle CLC based power plant lay-out  
733 with provisions for, with CCS and, without CCS modes  
734  
735  
736

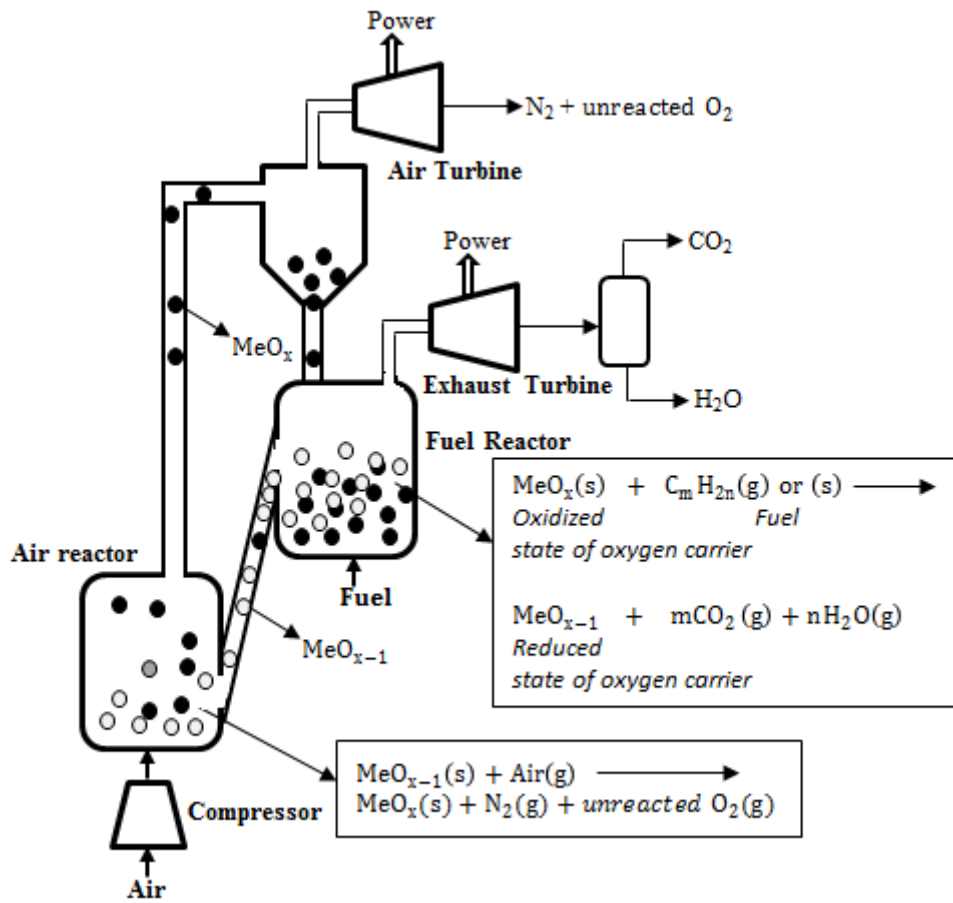
737 **LIST OF TABLES**

738 Table 1: Detailed thermodynamic analysis of natural gas fueled 761 MW<sub>th</sub> combined cycle chemical-  
739 looping combustion power plant  
740

741 Table 2: Detailed thermodynamic analysis of syngas fueled 800 MW<sub>th</sub> combined cycle chemical-  
742 looping combustion  
743

744 Table 3: Energy analysis of combined cycle CLC based power plants operating in CCS and non CCS  
745 modes  
746

747 Table 4: Overall energy analysis for combined cycle CLC  
748



749

750

Figure 1: Schematic illustration of pressurized chemical-looping combustion

751

752

753

754

755

756

757

758

759

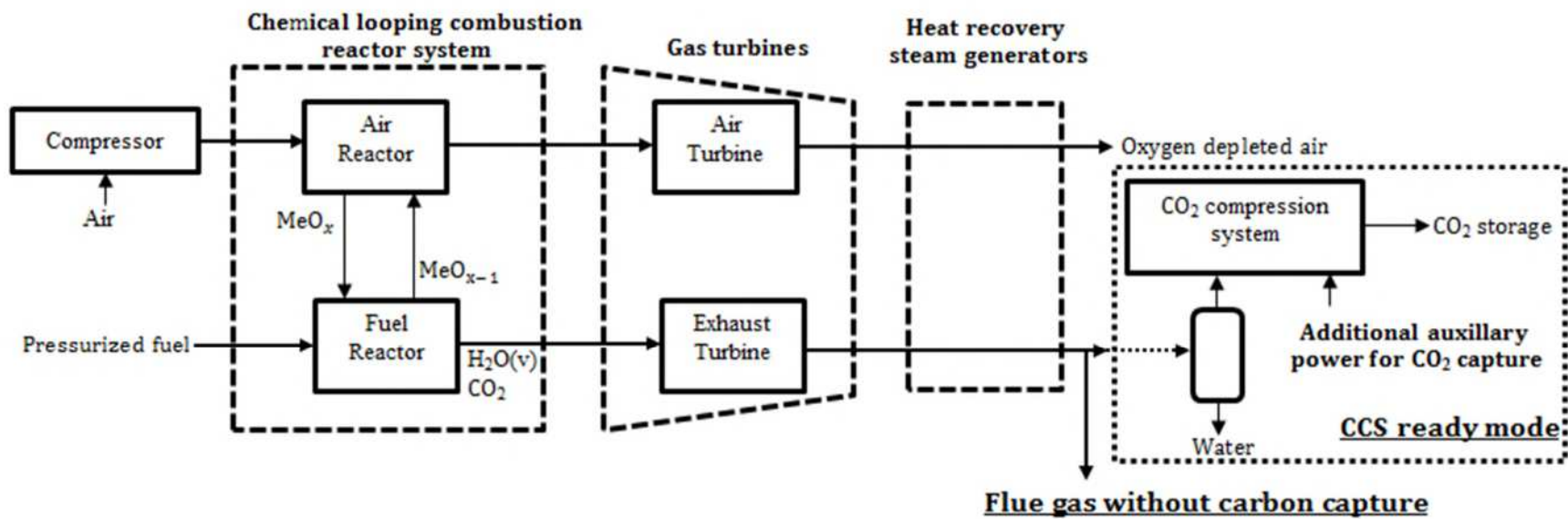
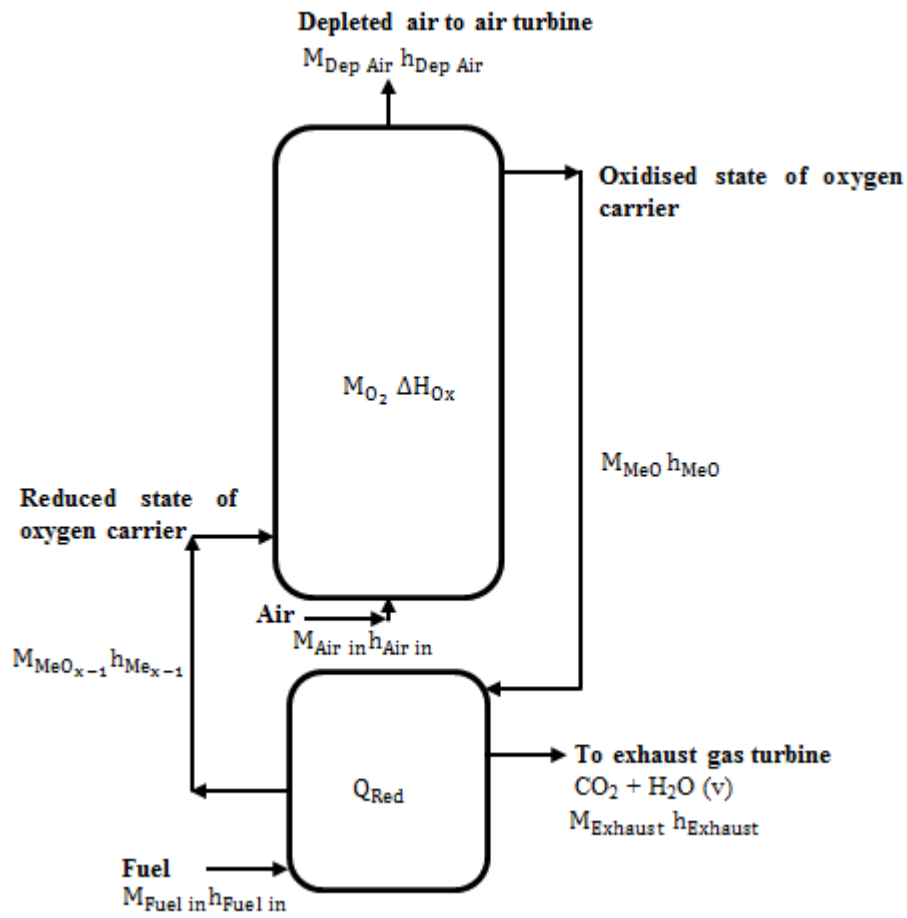


Figure 2: Schematic of flue gas handling in proposed chemical-looping combustion based power plant

760  
761  
762  
763  
764  
765  
766  
767  
768  
769  
770  
771  
772  
773  
774

775



776

777

Figure 3: Schematic of energy flow in combined cycle chemical-looping combustion

778

779

780

781

782

783

784

785

786

787

788

789



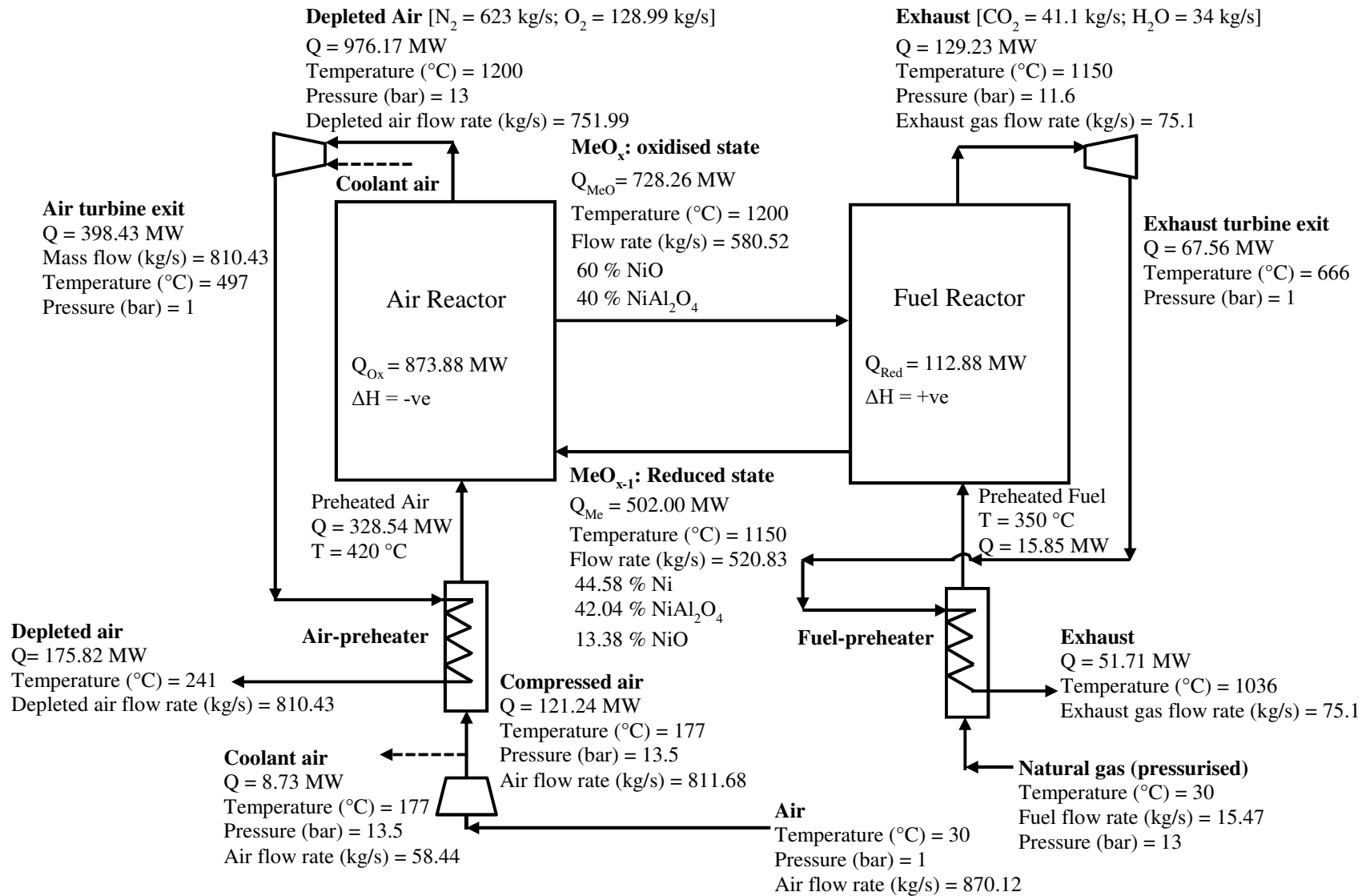


Figure 5 Furnace side heat balance of 761 MW<sub>th</sub> natural gas fueled combined cycle chemical looping combustion



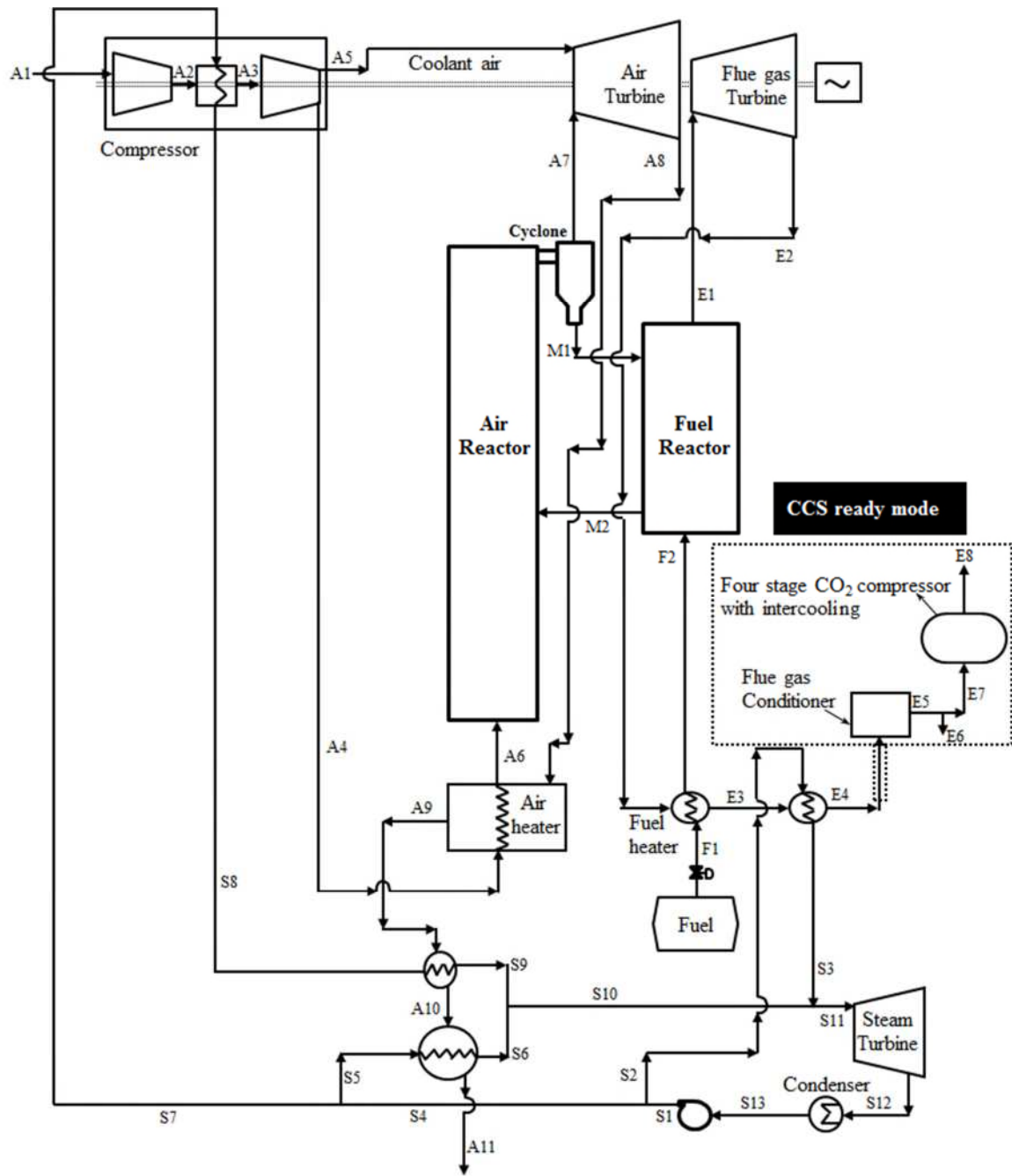


Figure 7: Schematic of natural gas fired 761 MW<sub>th</sub> combined cycle chemical-looping combustion power plant with provision of carbon capture

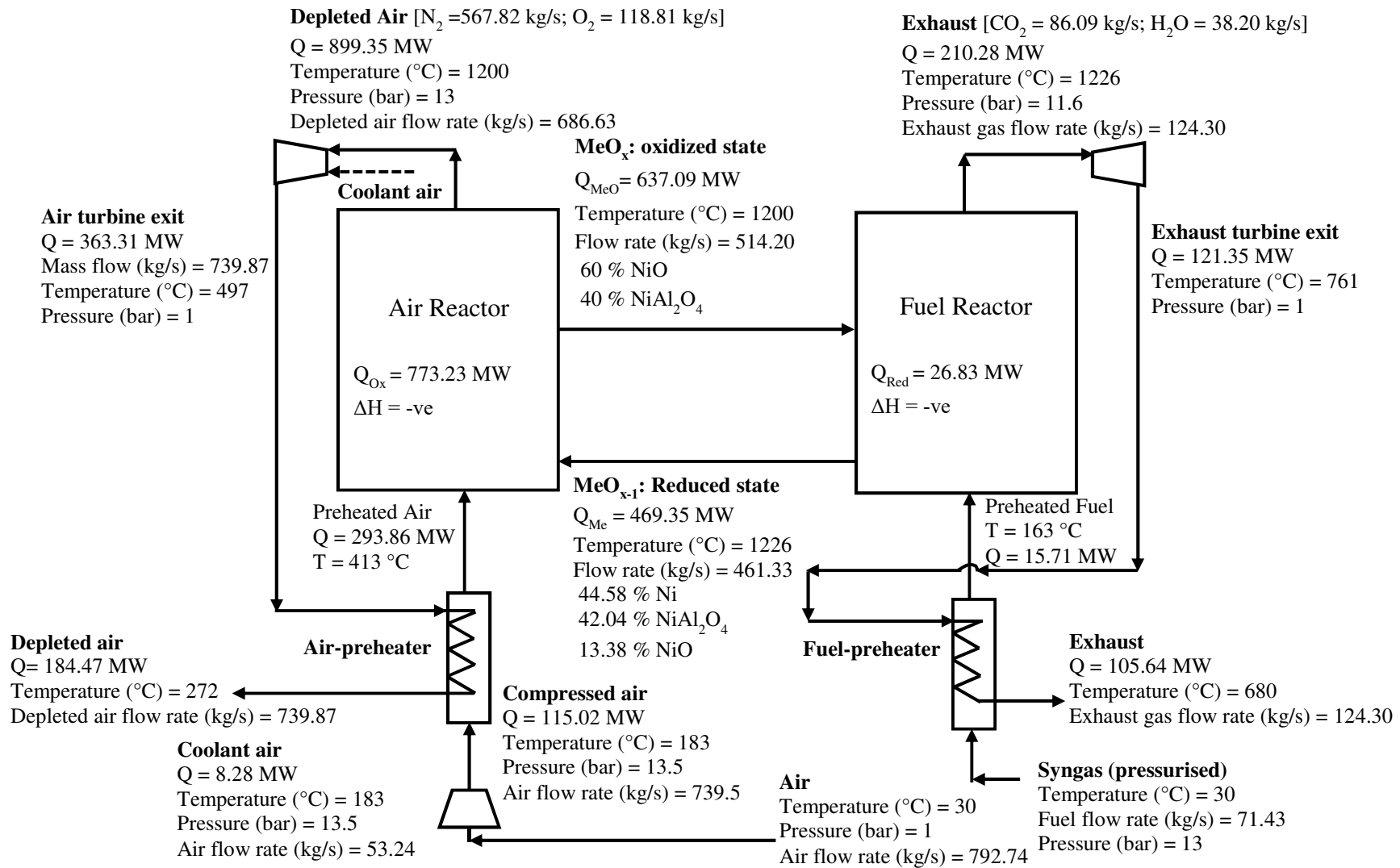


Figure 8: Furnace side heat balance for 800 MW<sub>th</sub> syngas fueled combined cycle CLC based power plant



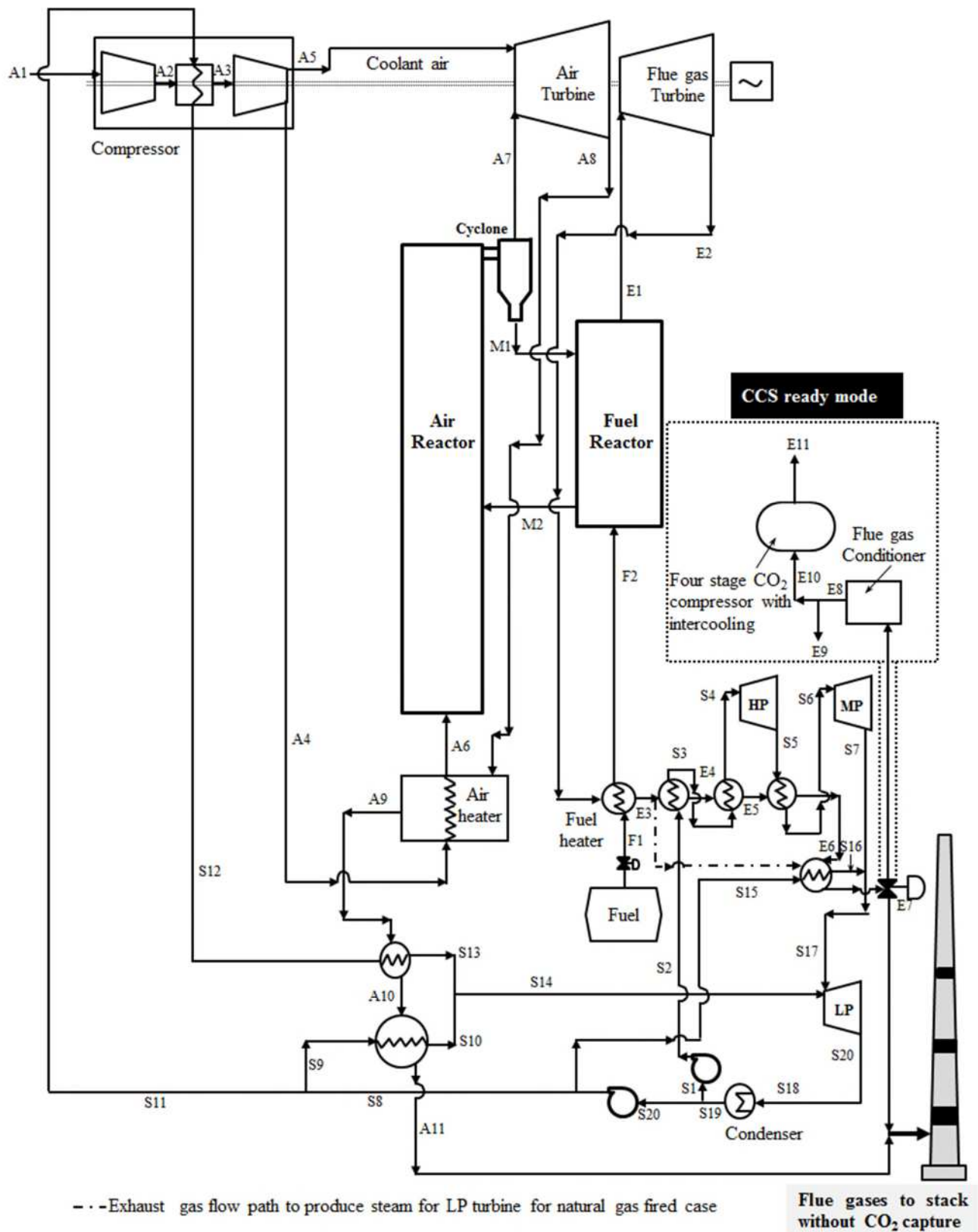


Figure 10: Schematic diagram of multi-fuel compatible combined cycle CLC based power plant layout with provisions for, with CCS and, without CCS modes

Table 1: Detailed thermodynamic analysis of natural gas fueled 761 MW<sub>th</sub> combined cycle chemical-looping combustion power plant

Stream	T (°C)	T (K)	P (bar)	m (kg/s)	h (kJ/kg)
Air					
A1	30	303.15	1.01	870.12	0.00
A2	152	425.15	3.43	870.12	123.71
A3	35	308.15	13.50	870.12	5.02
A4	177	450.15	13.50	811.68	149.37
A5	177	450.15	13.50	58.44	149.37
A6	420	693.15	13.50	811.68	404.77
A7	1200	1473.15	13.00	751.99	1298.12
A8	497	770.15	1.01	810.43	491.62
A9	241	514.15	1.01	810.43	216.94
A10	234	507.15	1.01	810.43	209.92
A11	74	347.15	1.01	810.43	44.34
Fuel					
F1	30	303.15	13.00	15.47	0.00
F2	350	623.15	13.00	15.47	1607.00
Exhaust					
E1	1150	1423.15	11.60	75.1	1720.79
E2	1036	1309.15	1.01	75.1	211.06
E3	463	736.15	1.01	75.1	568.26
E4	128	401.15	1.01	75.1	72.03
E5	40	313.15	1.01	75.1	23.56
E6	40	313.15	1.05	34	41.72
E7	40	313.15	1.05	41.1	8.54
E8	35	308.15	110.00	41.1	4.26
Oxygen carrier					
M1	1200	1473.15	13.00	580.52	1254.49
M2	1150	1423.15	11.60	520.83	963.85
Steam/water					
S1	31	304.15	1.70	104.81	4.17
S2	31	304.15	1.70	18.13	4.17
S3	190	463.15	1.70	13.07	2852.17
S4	31	304.15	1.70	86.68	4.17
S5	31	304.15	1.70	46.95	4.17
S6	190	463.15	1.70	46.95	2852.17
S7	31	304.15	1.70	39.73	4.17
S8	120	393.15	1.70	39.73	2709.16
S9	190	463.15	1.70	39.73	2852.17
S10	190	463.15	1.70	86.68	2852.17
S11	190	463.15	1.70	104.81	2852.17
S12	39	312.15	0.07	104.81	2571.70
S13	30	303.15	1.01	104.81	0.00

Table 2: Detailed thermodynamic analysis of syngas fueled 800 MW<sub>th</sub> combined cycle chemical-looping combustion

Stream	T (°C)	T (K)	P (bar)	m (kg/s)	h (kJ/kg)	Stream	T (°C)	T (K)	P (bar)	m (kg/s)	h (kJ/kg)
Air						Oxygen carrier					
A1	30	303.15	1.01	792.74	0.00	M1	1200	1473.15	13	514.20	1238.99
A2	152	425.15	3.43	792.74	123.71	M2	1226	1499.15	11.6	461.33	1017.38
A3	35	308.15	13.5	792.74	5.02	Steam/water					
A4	183	456.15	13.5	739.50	155.54	S1	30	303.15	1.01	9.64	0.00
A5	183	456.15	13.5	53.24	155.54	S2	31	304.15	150	9.64	4.18
A6	413	686.15	13.5	739.50	397.37	S3	185	458.15	150	9.64	792.24
A7	1200	1473.15	13	686.63	1309.80	S4	450	723.15	150	9.64	3157.84
A8	497	770.15	1.01	739.87	491.04	S5	325	598.15	20	9.64	3081.50
A9	272	544.94	1.01	739.87	249.32	S6	470	743.15	20	9.64	3402.01
A10	266	539.15	1.01	739.87	243.07	S7	190	463.15	1.7	9.64	2852.17
A11	75	348.15	1.01	739.87	45.71	S8	31	304.15	1.7	86.97	4.18
Fuel						S9	31	304.15	1.7	50.97	4.18
F1	30	303.15	13	71.43	0.00	S10	190	463.15	1.7	50.97	2852.17
F2	163	436.15	13	71.43	219.96	S11	31	304.15	1.7	36.00	4.18
Exhaust						S12	127	400.15	1.7	36.00	2723.90
E1	1226	1499.15	11.8	124.30	1691.73	S13	190	463.15	1.7	36.00	2852.17
E2	761	1034.15	1.01	124.30	976.25	S14	190	463.15	1.7	86.97	2852.17
E3	680	953.15	1.01	124.30	849.85	S15	31	304.15	1.7	21.93	4.18
E4	640	913.15	1.01	124.30	788.41	S16	190	463.15	1.7	21.93	2852.17
E5	517	790.15	1.01	124.30	604.96	S17	190	463.15	1.7	31.57	2852.17
E6	500	773.15	1.01	124.30	580.09	S18	39	312.15	0.069	118.54	2571.79
E7	128	401.15	1.01	124.30	76.98	S19	30	303.15	1	118.54	0.00
E8	40	313.15	1.01	124.30	23.56	S20	30	303.15	1	108.90	0.00
E9	40	313.15	1.05	38.20	41.72						
E10	40	313.15	1.05	86.09	8.54						
E11	35	308.15	110	86.09	4.26						

Table 3: Energy analysis of combined cycle CLC based power plants operating in CCS and non CCS modes

<b>Power produced/consumed</b>	<b>Natural gas CC CLC</b>		<b>Syngas CC CLC</b>	
	<b>CCS Mode</b>	<b>Non CCS Mode</b>	<b>CCS Mode</b>	<b>Non CCS Mode</b>
<i>Power produced</i>				
Air turbine (kW <sub>e</sub> )	596,064	596,064	544,302	544,302
Carbon dioxide rich gas turbine (kW <sub>e</sub> )	61,674	61,674	88,934	889,34
Steam turbine power (kW <sub>e</sub> )	29,396	29,396	39,253	39,253
<i>Power consumed</i>				
Air compression (kW <sub>e</sub> )	275,716	275,716	251,197	251,197
<b>CO<sub>2</sub> compression to 110 bar (kW<sub>e</sub>)</b>	<b>14,721</b>	-	<b>30,842</b>	-
Water pump cost (kW <sub>e</sub> )	10	10	202	202
<i>Available power (kW<sub>e</sub>)</i>				
Available power (kW <sub>e</sub> )	396,6877	411,408	390,248	421,091
Thermal input (kW <sub>e</sub> )	761,000	761,000	800,061	800,061
<b>Net Efficiency (%)</b>	52.13	54.06	48.78	52.63

Table 4: Overall energy analysis for combined cycle CLC

<b>Comparative analyses of Combined Cycle Chemical Looping combustion power plants</b>			
<i>Variants</i>	<i>Syngas Lay-out</i>	<i>Natural gas lay-out</i>	<i>Natural gas lay-out (Naqvi, 2007)</i>
Air reactor operating temperature (°C)	1200	1200	1200
Fuel reactor operating temperature (°C)	1226	1150	980
Temperature of 13 bar pressure oxygen depleted air at air turbine inlet (°C)	1132	1132	1140
Temperature of 1 bar pressure oxygen depleted air at air turbine exit (°C) (at 92% isentropic efficiency)	497	497	492
CLC fuel reactor exhaust gas turbine inlet temperature (°C) at pressure 11.6 bar	1226	1150	980
CLC fuel reactor exhaust exit temperature (°C) at 1 bar (at 92% isentropic efficiency)	761	666	533
Mass flow rate of depleted air at air turbine inlet/exit after addition of coolant air in CC CLC (kg/s)	739.87	810.43	768
Mass flow rate of fuel reactor exhaust gas at exhaust gas inlet/exit in CC CLC (kg/s)	124.30	75.1	70.5
CLC Air turbine inlet/exit gas composition (wt %)	82.7 % N <sub>2</sub> and 17.3 % O <sub>2</sub>	82.85 % N <sub>2</sub> and 17.15% O <sub>2</sub>	83 % N <sub>2</sub> and 17 % O <sub>2</sub>
CLC exhaust gas turbine inlet/exit gas composition (wt %)	30.63 % H <sub>2</sub> O and 69.37 % CO <sub>2</sub>	45.32 % H <sub>2</sub> O and 54.68 % CO <sub>2</sub>	45.32 % H <sub>2</sub> O and 54.68 % CO <sub>2</sub>
CO <sub>2</sub> purity (wt %) for CCS	>99	>99	99
<i>Power produced</i>			
Air turbine (kW <sub>e</sub> )	544,302	596,064	477,000
Carbon dioxide rich gas turbine (kW <sub>e</sub> )	88,934	61,674	53,600
Steam cycle	150 bar at 450°C (736 kW), 20 bar at 470°C (5,301.5 kW) 1.7 bar at 190°C (33,216 kW)	1.7 bar at 190°C	60 bar at 467°C, 5 bar at 258°C
Steam turbine power (kW <sub>e</sub> )	39,253	29,396	101,000
<i>Power consumed</i>			
Air compression (kW <sub>e</sub> )	251,197	275,716	243,000
CO <sub>2</sub> compression (kW <sub>e</sub> ) (Compressor efficiency 85%)	30,842 (to 110 bar)	14,721 (to 110 bar)	15,400 (to 200 bar)
Water circulation cost (kW <sub>e</sub> ) (Pump efficiency 75%)	202 (1 to 150 bar)	10 (1 to 1.7 bar)	-
Available power (kW <sub>e</sub> )	390,248	395,267	364,000
Thermal input (kW)	800,061	761,000	697,545
Net Efficiency (%)	48.78	52.13	52.18